

ELECTRONIC SUPPLEMENTARY INFORMATION FOR

# **Semiconducting Liquid Crystalline Dispersions with Precisely Adjustable Band Gaps and Polarized Photoluminescence**

Tingting Zhou,<sup>1,2</sup> Penghao Guo,<sup>1,2</sup> Xuelian Jiang,<sup>1,2</sup> Hongbo Zhao,<sup>1,2</sup> Qing Zhang,<sup>3</sup> Pei-Xi Wang<sup>1,2\*</sup>

<sup>1</sup> School of Nano-Tech and Nano-Bionics, University of Science and Technology of China, 96 Jinzhai Road, Hefei, Anhui, 230026, P. R. China

<sup>2</sup> i-Lab, Suzhou Institute of Nano-Tech and Nano-Bionics of the Chinese Academy of Sciences, 398 Ruoshui Road, Suzhou Industrial Park, Suzhou, Jiangsu, 215123, P. R. China

<sup>3</sup> NANO-X Vacuum Interconnected Nanotech Workstation, Suzhou Institute of Nano-Tech and Nano-Bionics of the Chinese Academy of Sciences, 385 Ruoshui Road, Suzhou Industrial Park, Suzhou, Jiangsu, 215123, P. R. China

\*Correspondence: pxwang2020@sinano.ac.cn

## EXPERIMENTAL METHODS

### Materials

Hydrochloric acid (37 wt.% in water, Sigma-Aldrich), hydrobromic acid (48 wt.% in water, Sigma-Aldrich), hydroiodic acid (57 wt.% in water, Sigma-Aldrich), manganese(II) acetate tetrahydrate (99%, Sigma-Aldrich), lead(II) oxide (99%, Sigma-Aldrich), n-butylamine (99.5%, Sigma-Aldrich), 2-phenylethylamine (99%, Sigma-Aldrich), phenylmethylamine (99%, Sigma-Aldrich), [(4-fluorophenyl)methyl]amine (97%, Sigma-Aldrich), [(4-chlorophenyl)methyl]amine (98%, Sigma-Aldrich), N,N-dimethylformamide (anhydrous, 99.8 %, Sigma-Aldrich), cis-9-octadecenoic acid (oleic acid; > 99.0 %, Sigma-Aldrich), cis-1-amino-9-octadecene (oleylamine; > 98.0 %, Sigma-Aldrich), chlorobenzene (anhydrous, 99.8 %, Sigma-Aldrich), and cyclohexane (anhydrous, 99.5 %, Sigma-Aldrich) were used as received.

### Characterization

Photoluminescence emission spectroscopy was conducted on a Hitachi F-4600 Fluorescence Spectrophotometer and the perovskite liquid crystalline dispersions were sealed in quartz cuvettes with an optical path length of 1 mm. Field emission scanning electron spectroscopy was performed on a Hitachi Regulus 8230 Ultra-high Resolution Scanning Electron Microscope. Atomic force microscopy was conducted on a Bruker Dimension Icon Atomic Force Microscope with ScanAsyst. Samples for SEM and AFM observations were prepared by spin-coating the colloidal lyotropic liquid crystalline dispersions of perovskite nanoplatelets (about 100 mg per mL in chlorobenzene) onto flat silicon (111) surfaces at a spinning speed of 6000 revolutions per minute for 60 seconds followed by thermal annealing at 373 K for 10 minutes. Excess surfactants on the samples were removed by immersion in a large volume (50 mL) of cyclohexane for about 30 minutes then dried in a nitrogen or argon atmosphere. Powder X-ray diffraction patterns were collected on a Bruker D8 ADVANCE Diffractometer using copper K-alpha radiation (with a wavelength of 0.15406 nm). Polarized optical microscopy images were obtained from a BM2100POL Polarized Optical Microscope.

Under White Light

Under 365-nm Ultraviolet Light

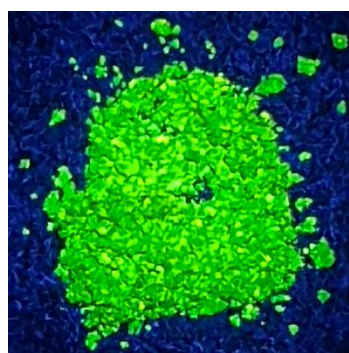
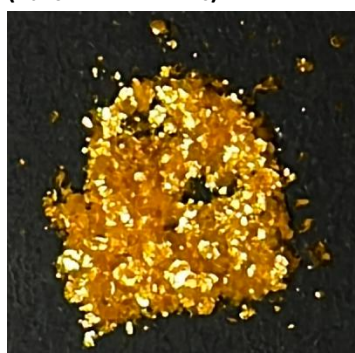
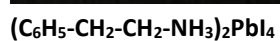
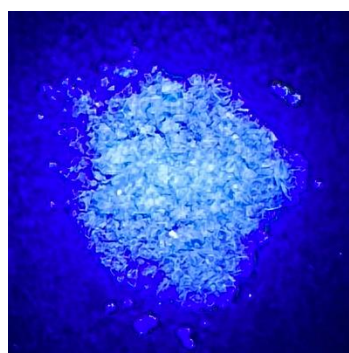
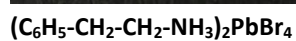
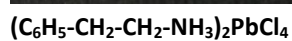
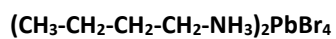


**Figure S1.** Photographs showing the synthesized two-dimensional organic-inorganic lead halide perovskite crystals of  $(\text{CH}_3\text{-CH}_2\text{-CH}_2\text{-CH}_2\text{-NH}_3)_2\text{PbBr}_4$ ,  $(\text{C}_6\text{H}_5\text{-CH}_2\text{-CH}_2\text{-NH}_3)_2\text{PbCl}_4$ ,  $(\text{C}_6\text{H}_5\text{-CH}_2\text{-CH}_2\text{-NH}_3)_2\text{PbBr}_4$ , and  $(\text{C}_6\text{H}_5\text{-CH}_2\text{-CH}_2\text{-NH}_3)_2\text{PbI}_4$ .

Under White Light

Under 365-nm Ultraviolet Light

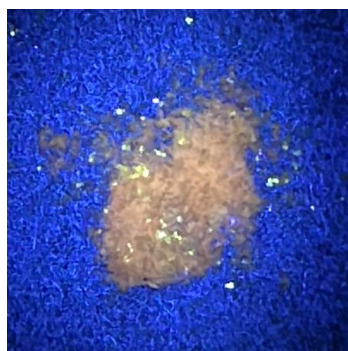
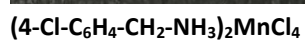
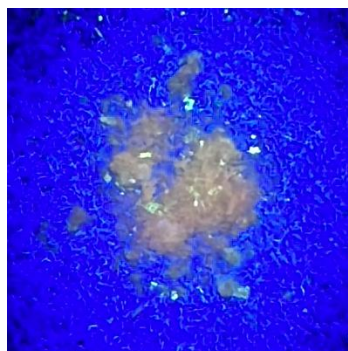
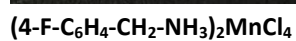
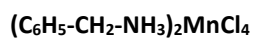


**Figure S2.** Photographs of the synthesized two-dimensional organic-inorganic manganese chloride perovskite crystals of  $(\text{C}_6\text{H}_5\text{-CH}_2\text{-NH}_3)_2\text{MnCl}_4$ ,  $(4\text{-F-C}_6\text{H}_4\text{-CH}_2\text{-NH}_3)_2\text{MnCl}_4$ , and  $(4\text{-Cl-C}_6\text{H}_4\text{-CH}_2\text{-NH}_3)_2\text{MnCl}_4$ , where photos in the left column were taken under white light, while photos in the right column were taken under ultraviolet light with a wavelength of 365 nanometers.



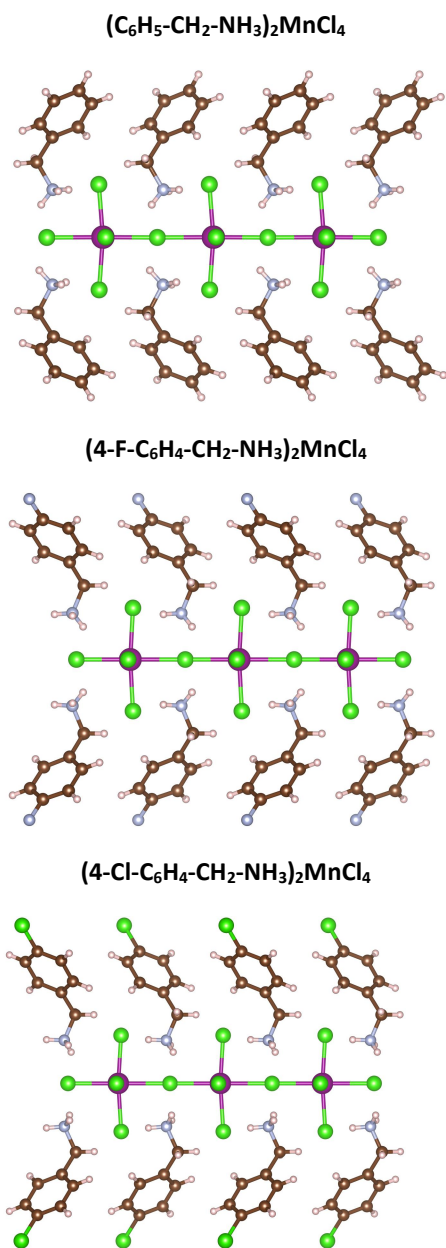


**Figure S3.** Crystal structures (obtained by single-crystal X-ray diffraction analysis) of perovskites (C<sub>6</sub>H<sub>5</sub>-CH<sub>2</sub>-NH<sub>3</sub>)<sub>2</sub>MnCl<sub>4</sub>, (4-F-C<sub>6</sub>H<sub>4</sub>-CH<sub>2</sub>-NH<sub>3</sub>)<sub>2</sub>MnCl<sub>4</sub>, and (4-Cl-C<sub>6</sub>H<sub>4</sub>-CH<sub>2</sub>-NH<sub>3</sub>)<sub>2</sub>MnCl<sub>4</sub>.

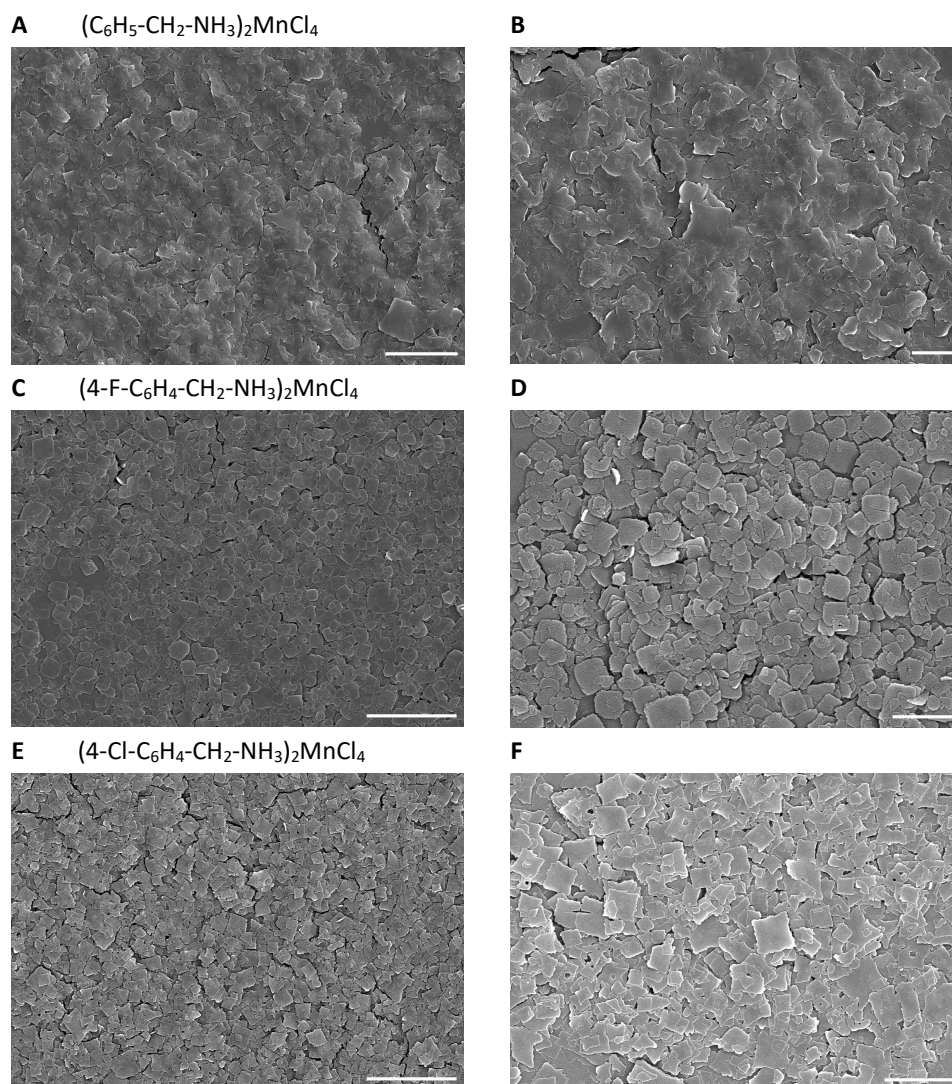


**Figure S4.** Scanning electron microscopy images showing plate-shaped colloidal nanocrystals of  $(\text{C}_6\text{H}_5\text{-CH}_2\text{-NH}_3)_2\text{MnCl}_4$  (**A,B**),  $(4\text{-F-C}_6\text{H}_4\text{-CH}_2\text{-NH}_3)_2\text{MnCl}_4$  (**C,D**), and  $(4\text{-Cl-C}_6\text{H}_4\text{-CH}_2\text{-NH}_3)_2\text{MnCl}_4$  (**E,F**). Scale bars: 5  $\mu\text{m}$  (**A,C,E**), 2  $\mu\text{m}$  (**B,D,F**).

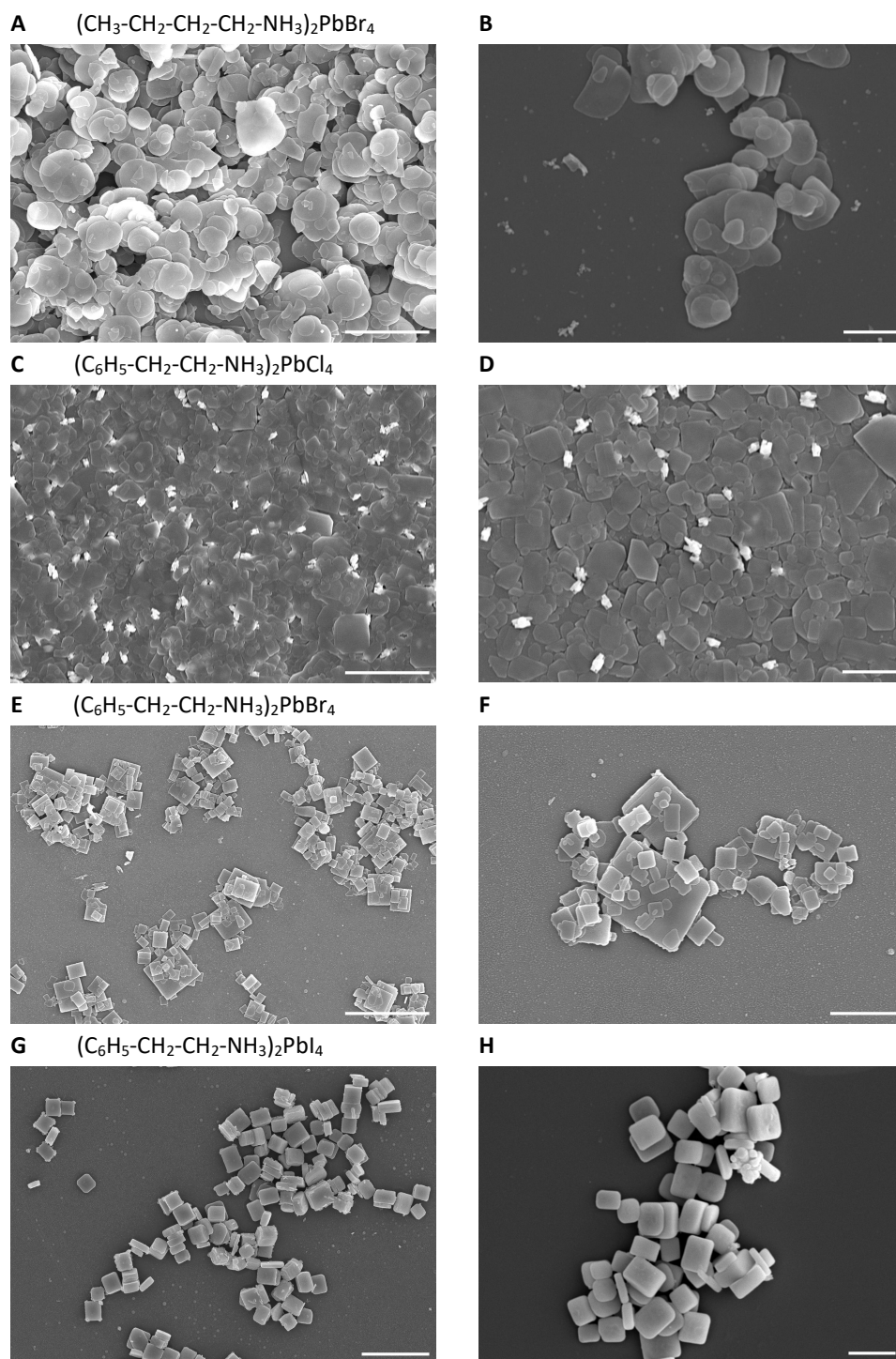


**Figure S5.** Scanning electron microscopy images of the colloidal nanoparticles of  $(\text{CH}_3\text{-CH}_2\text{-CH}_2\text{-CH}_2\text{-NH}_3)_2\text{PbBr}_4$  (**A,B**),  $(\text{C}_6\text{H}_5\text{-CH}_2\text{-CH}_2\text{-NH}_3)_2\text{PbCl}_4$  (**C,D**),  $(\text{C}_6\text{H}_5\text{-CH}_2\text{-CH}_2\text{-NH}_3)_2\text{PbBr}_4$  (**E,F**), and  $(\text{C}_6\text{H}_5\text{-CH}_2\text{-CH}_2\text{-NH}_3)_2\text{PbI}_4$  (**G,H**). Scale bars: 5  $\mu\text{m}$  (**A,C,E,G**), 2  $\mu\text{m}$  (**B,D,F,H**).

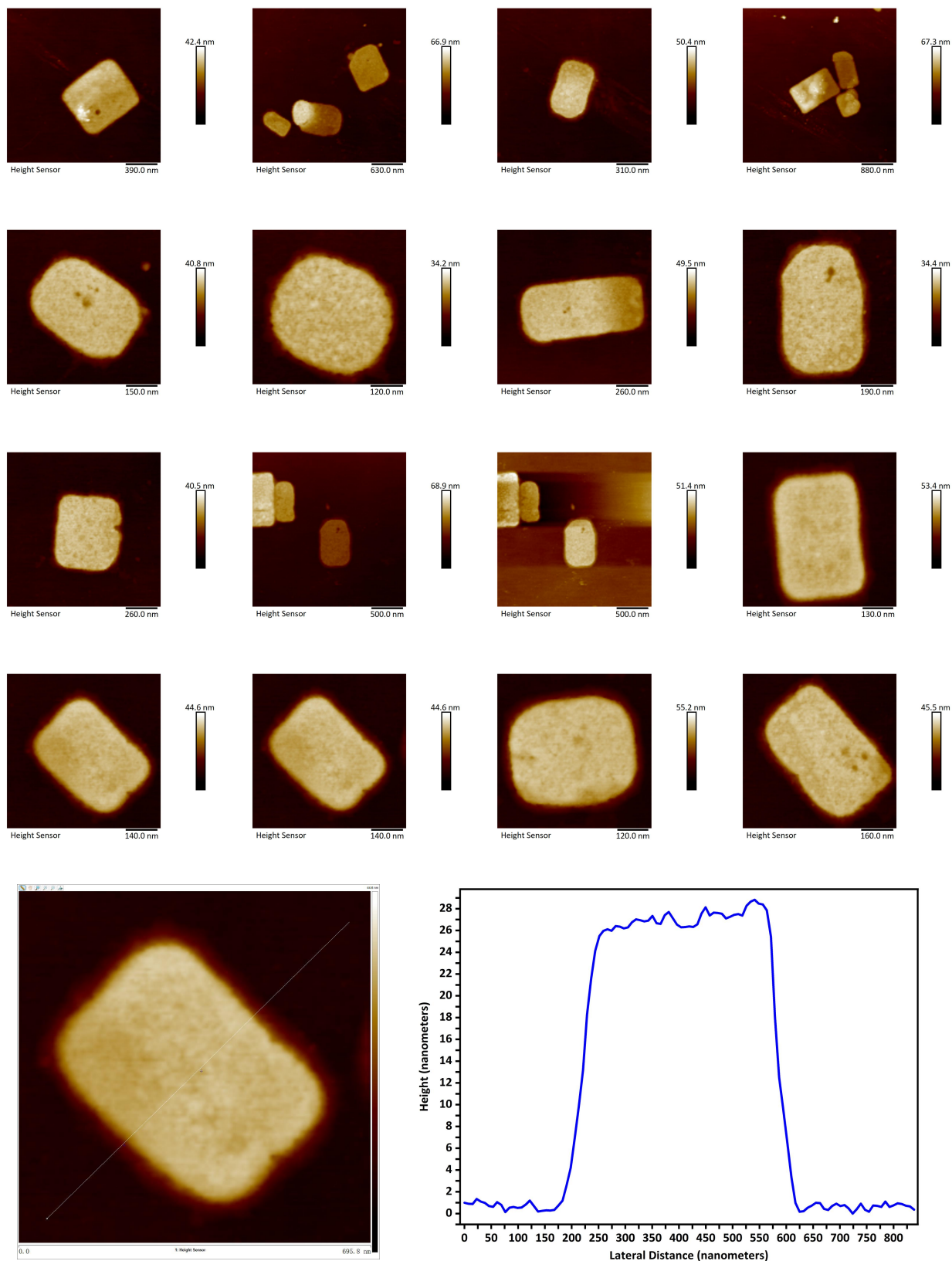


**Figure S6.** Atomic force microscopy images and height profiles showing lateral dimensions and thicknesses of different  $(\text{C}_6\text{H}_5\text{-CH}_2\text{-CH}_2\text{-NH}_3)_2\text{PbBr}_4$  perovskite nanoplatelets.

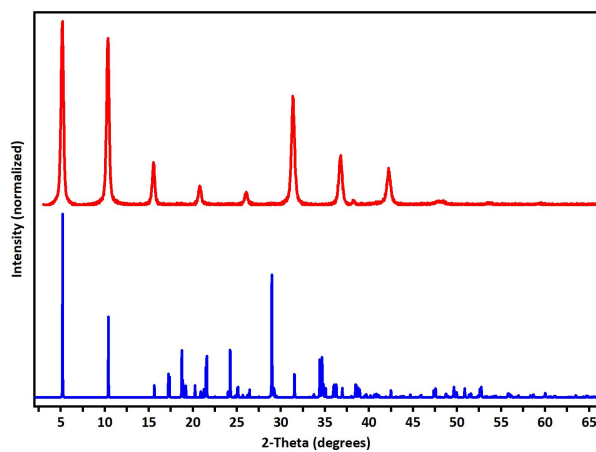
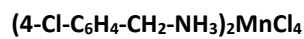
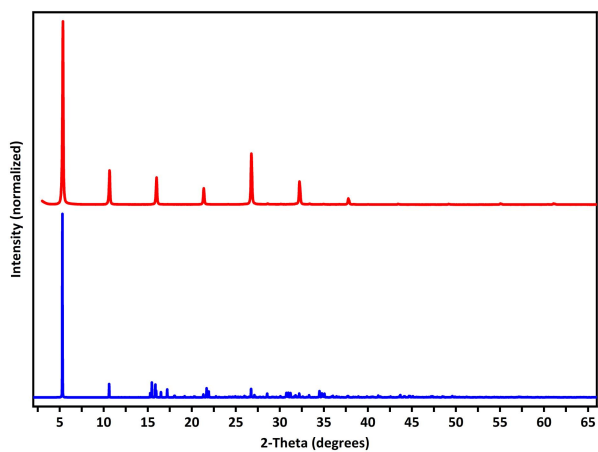
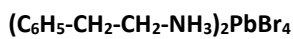
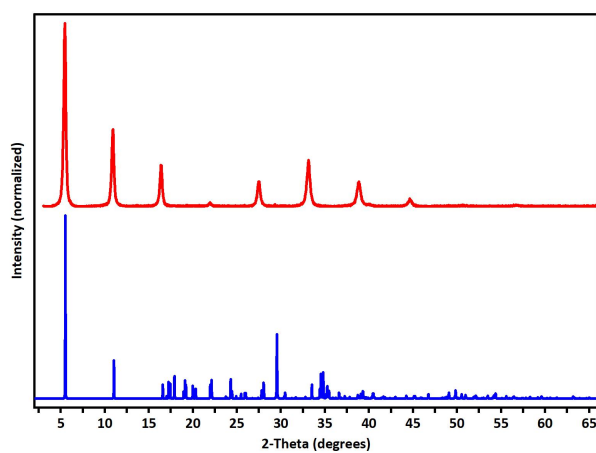
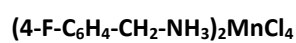
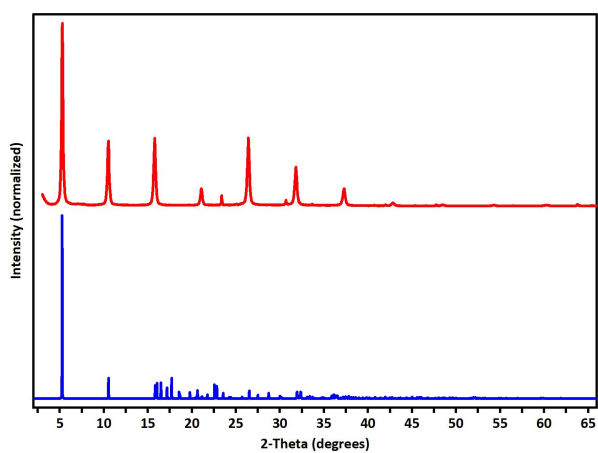
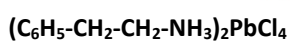
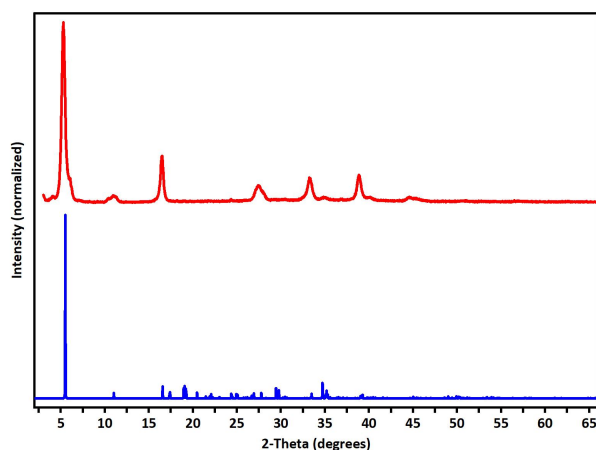
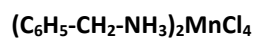
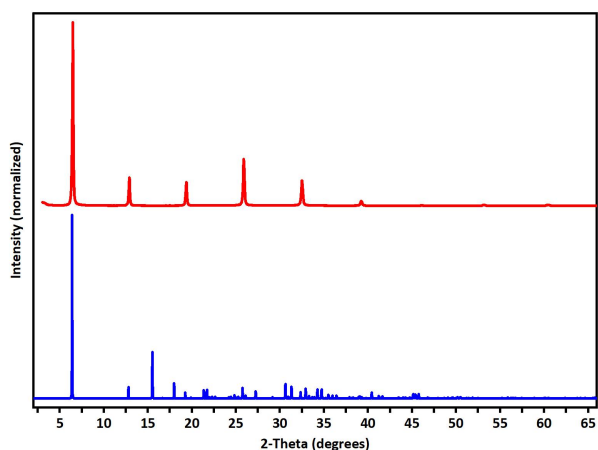
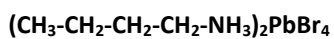


**Figure S7.** Powder X-ray diffraction patterns obtained by experimental measurements of spin-coated and dried thin films of colloidal liquid crystalline dispersions of perovskite nanoplatelets (upper red curves) and by simulations based on corresponding single-crystal X-ray diffraction data (lower blue curves).



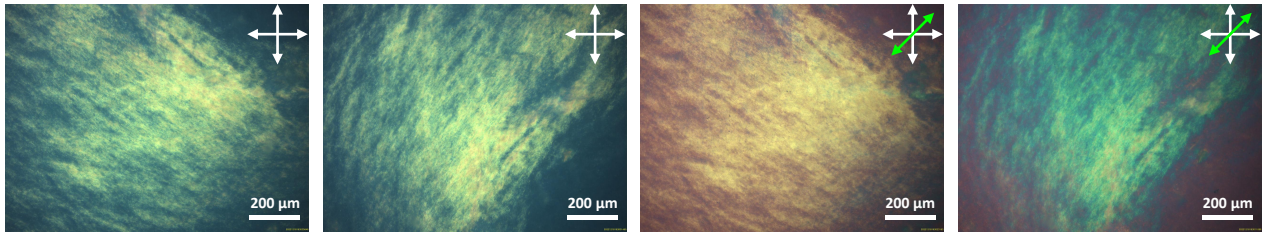
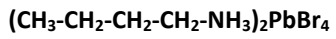
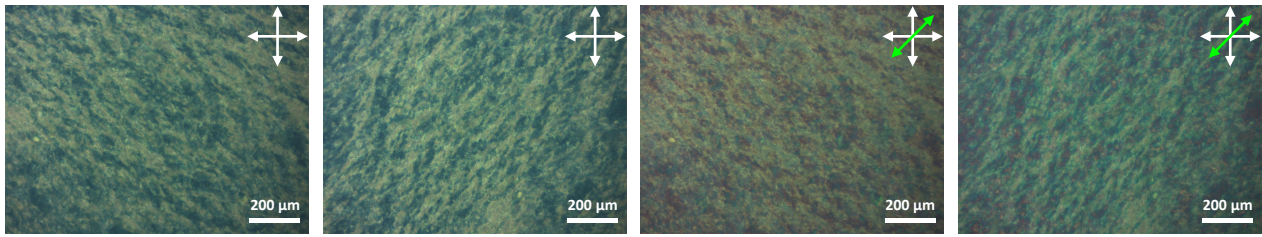
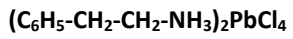


**Figure S8.** Polarized optical microscopy images showing the liquid crystalline phases formed by colloidal nanoplatelets of two-dimensional lead(II) halide perovskites. These samples were observed between two perpendicularly oriented linear polarizers (the left two columns) and with a 530-nm full-wavelength retardation plate (the right two columns).

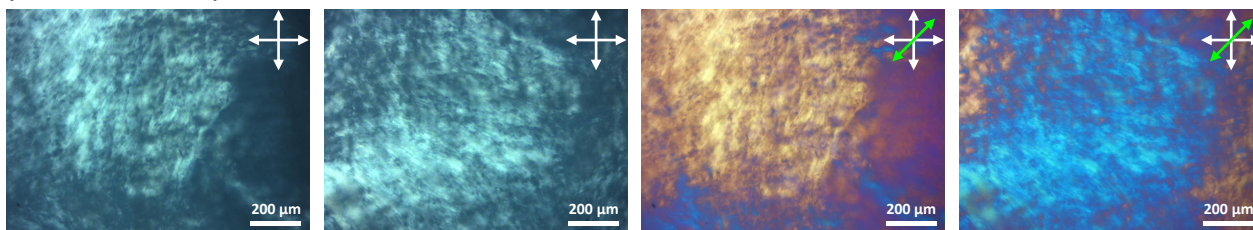
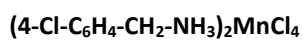
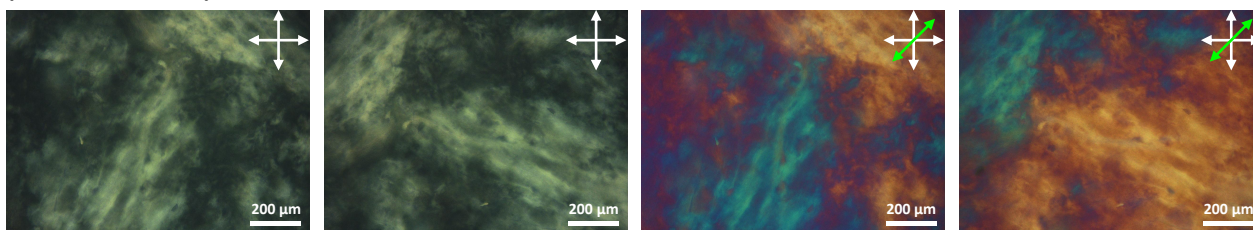
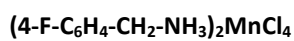
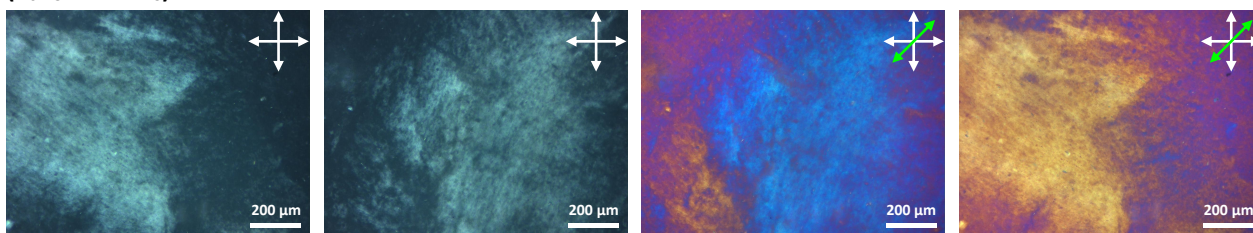
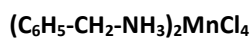


**Figure S9.** Polarized optical microscopy images showing the liquid crystalline phases formed by colloidal nanoplatelets of two-dimensional organic-inorganic manganese(II) chloride perovskites. In the left two columns, the samples were observed between two perpendicularly oriented linear polarizers; in the right two columns, a 530-nm full-wavelength retardation plate was inserted into the optical path.

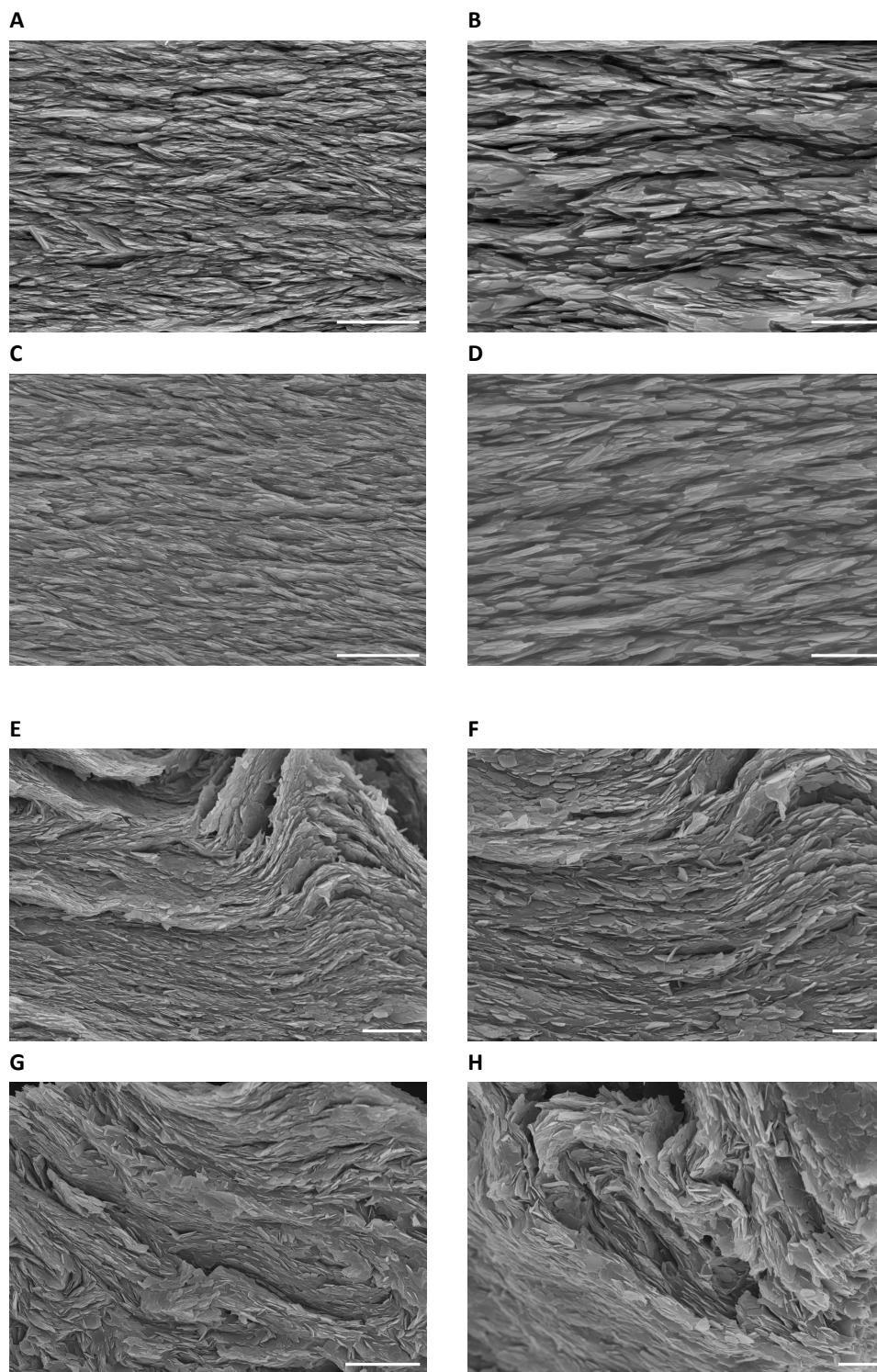


**Figure S10.** Cross-sectional scanning electron microscopy images showing the discotic nematic liquid crystalline phases formed by colloidal nanoplatelets of  $(\text{C}_6\text{H}_5\text{-CH}_2\text{-CH}_2\text{-NH}_3)_2\text{PbBr}_4$  (**A-D**) and  $(4\text{-F-C}_6\text{H}_4\text{-CH}_2\text{-NH}_3)_2\text{MnCl}_4$  (**E-H**). Scale bars: 5  $\mu\text{m}$  (**A,C,E,G**), 2  $\mu\text{m}$  (**B,D,F,H**).

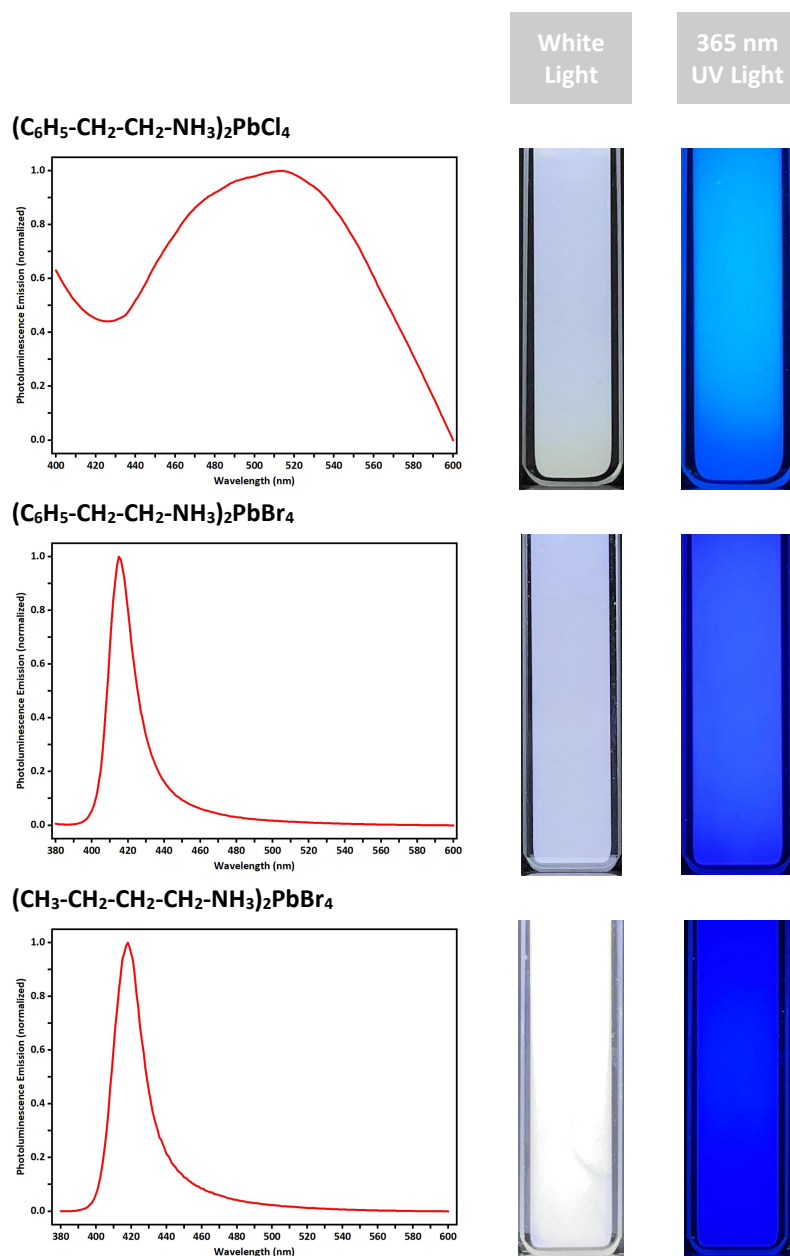
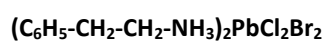
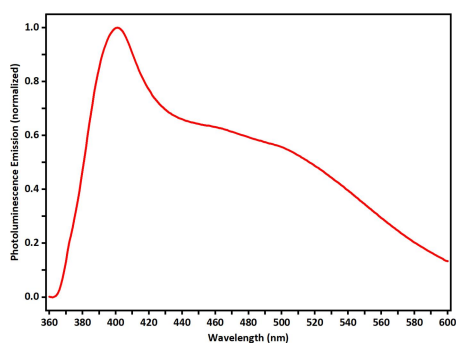


**Figure S11.** Photoluminescence emission spectra of the crystalline powders (red curves) and colloidal liquid crystalline dispersions (blue curves) of  $(\text{C}_6\text{H}_5\text{-CH}_2\text{-CH}_2\text{-NH}_3)_2\text{PbCl}_4$ ,  $(\text{C}_6\text{H}_5\text{-CH}_2\text{-CH}_2\text{-NH}_3)_2\text{PbBr}_4$ , and  $(\text{CH}_3\text{-CH}_2\text{-CH}_2\text{-CH}_2\text{-NH}_3)_2\text{PbBr}_4$ . Photographs of these liquid crystals (sealed in quartz cuvettes with an internal width of 10 mm and an optical path length of 0.5 mm, observed under white light and 365-nm ultraviolet light) are displayed next to the spectra plots.

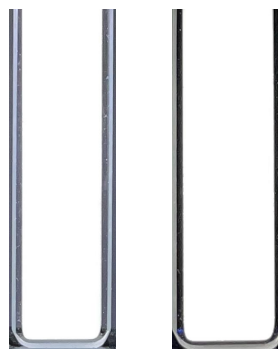


### Photoluminescence Emission Spectrum



White  
Light

365 nm  
UV Light



### Powder X-ray Diffraction Patterns

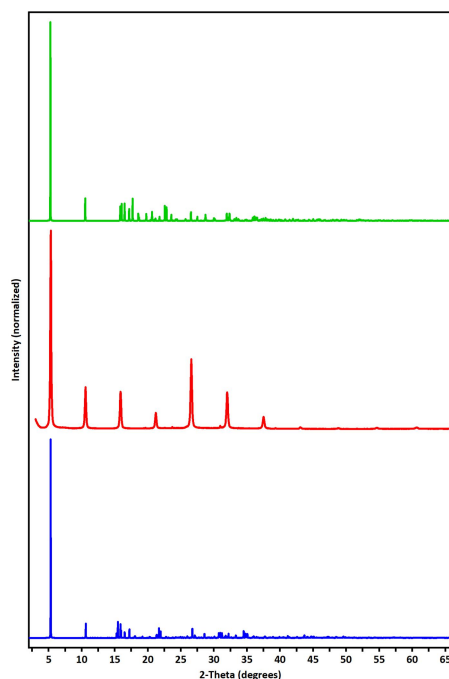


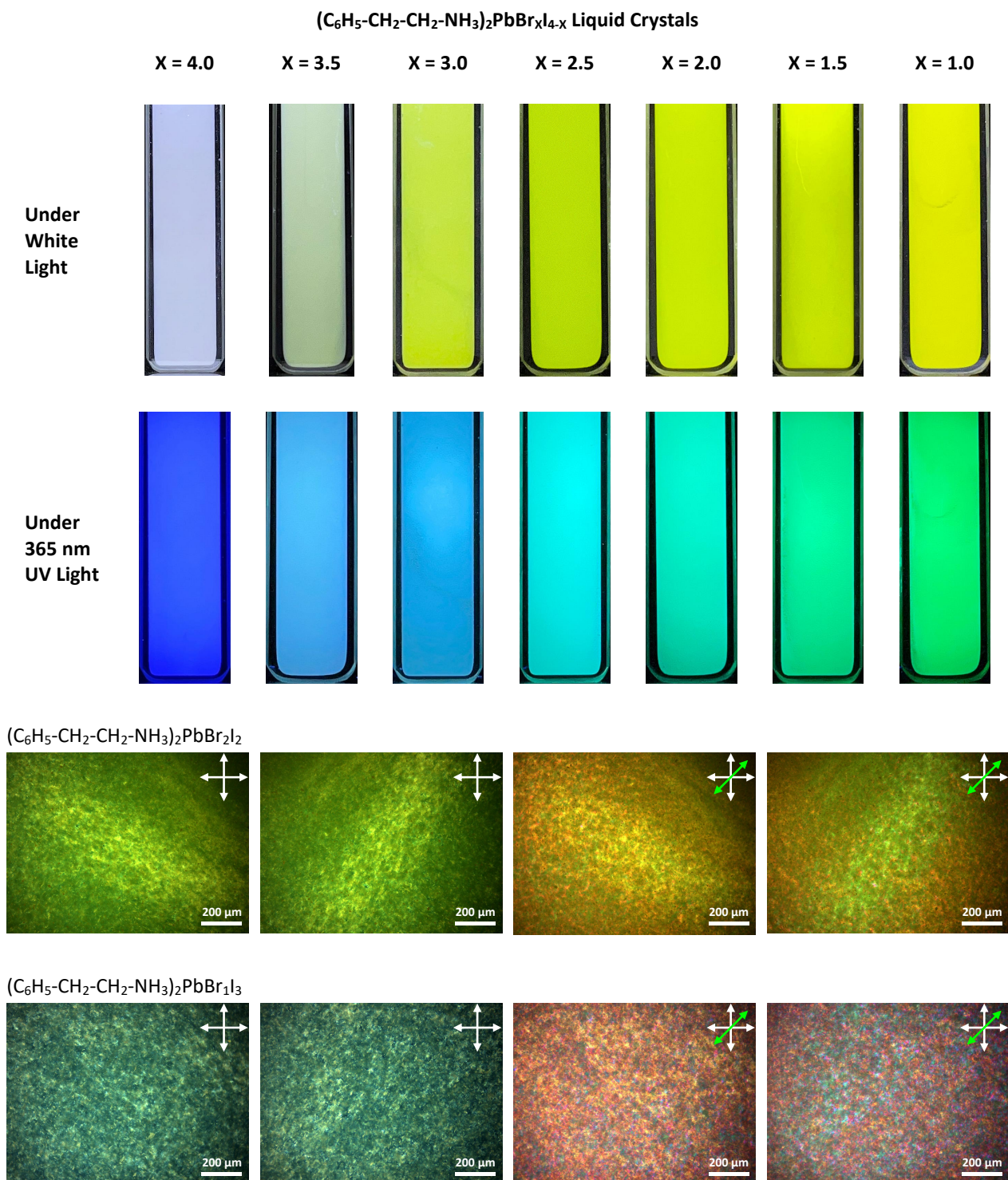
**Figure S12.** Additional data for liquid crystalline dispersions of  $(\text{C}_6\text{H}_5\text{-CH}_2\text{-CH}_2\text{-NH}_3)_2\text{PbCl}_2\text{Br}_2$  perovskite nanocrystals:

(1) Photoluminescence emission spectrum.

(2) Photographs. The liquid crystal was sealed in a quartz cuvette with an internal width of 10 mm and an optical path length of 0.5 mm. The photos were taken under white light and 365-nm ultraviolet light.

(3) Powder X-ray diffraction pattern of a spin-coated and dried film of the liquid crystal (middle red curve). Simulated PXRD patterns (based on single-crystal X-ray diffraction profiles) of  $(\text{C}_6\text{H}_5\text{-CH}_2\text{-CH}_2\text{-NH}_3)_2\text{PbCl}_4$  (upper green curve) and  $(\text{C}_6\text{H}_5\text{-CH}_2\text{-CH}_2\text{-NH}_3)_2\text{PbBr}_4$  (lower blue curve) are also displayed for comparison.

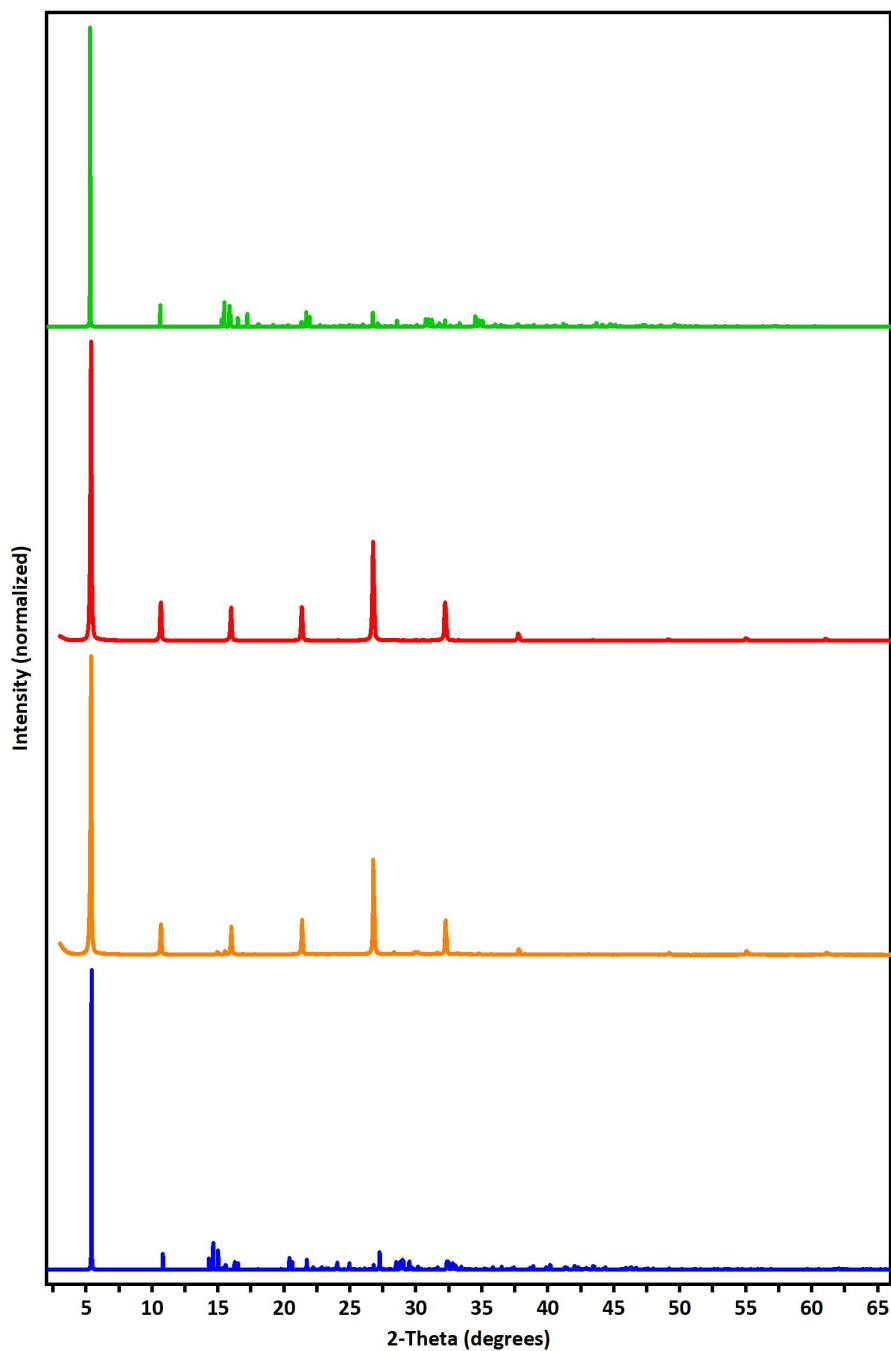




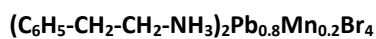
**Figure S13.** Additional data for  $(\text{C}_6\text{H}_5\text{-CH}_2\text{-CH}_2\text{-NH}_3)_2\text{PbBr}_{x\text{I}_{4-x}}$  liquid crystals:

(1) Photographs. The liquid crystal was sealed in a quartz cuvette with an internal width of 10 mm and an optical path length of 0.5 mm. The photos were taken under white light and 365-nm ultraviolet light.

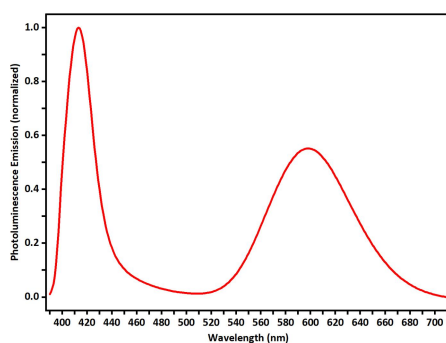
(2) Polarized optical microscopy images.



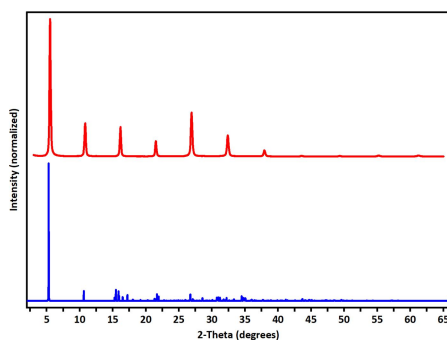
**Figure S14.** Powder X-ray diffraction patterns of spin-coated and dried films of colloidal liquid crystalline dispersions of  $(\text{C}_6\text{H}_5\text{-CH}_2\text{-CH}_2\text{-NH}_3)_2\text{PbBr}_2\text{I}_2$  (red-colored curve) and  $(\text{C}_6\text{H}_5\text{-CH}_2\text{-CH}_2\text{-NH}_3)_2\text{PbBr}_3\text{I}$  (orange-colored curve) perovskites. Simulated PXRD patterns (based on single-crystal X-ray diffraction profiles) of  $(\text{C}_6\text{H}_5\text{-CH}_2\text{-CH}_2\text{-NH}_3)_2\text{PbBr}_4$  (green-colored curve at the top) and  $(\text{C}_6\text{H}_5\text{-CH}_2\text{-CH}_2\text{-NH}_3)_2\text{PbI}_4$  (blue-colored curve at the bottom) are also displayed for comparison.

White  
Light365 nm  
UV Light

## Photoluminescence Emission Spectrum



## Powder X-ray Diffraction Patterns



## Polarized Optical Microscopy Images

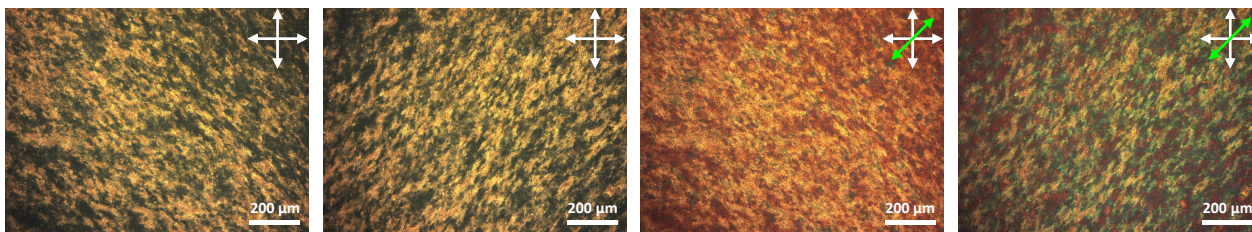


**Figure S15.** Additional data for  $(\text{C}_6\text{H}_5\text{-CH}_2\text{-CH}_2\text{-NH}_3)_2\text{Pb}_{0.8}\text{Mn}_{0.2}\text{Br}_4$  perovskite liquid crystals:

(1) Photoluminescence emission spectrum.

(2) Photographs. The liquid crystal was sealed in a quartz cuvette with an internal width of 10 mm and an optical path length of 0.5 mm. The photos were taken under white light and 365-nm ultraviolet light.

(3) Powder X-ray diffraction pattern of a spin-coated and dried film of the liquid crystal (red curve). The simulated PXRD pattern (based on single-crystal XRD data) of  $(\text{C}_6\text{H}_5\text{-CH}_2\text{-CH}_2\text{-NH}_3)_2\text{PbBr}_4$  (blue curve) is displayed for comparison.

(4) Polarized optical microscopy images.

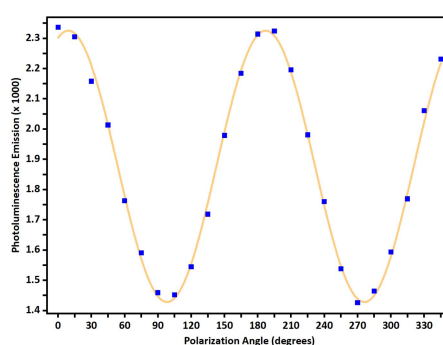
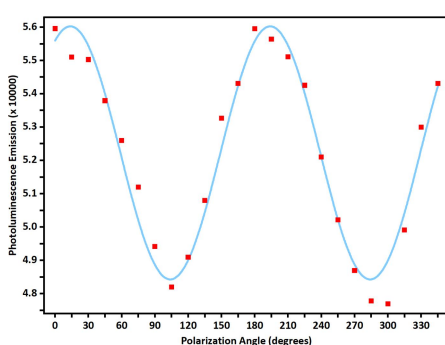
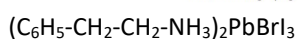
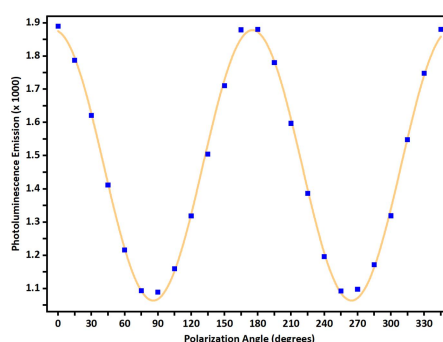
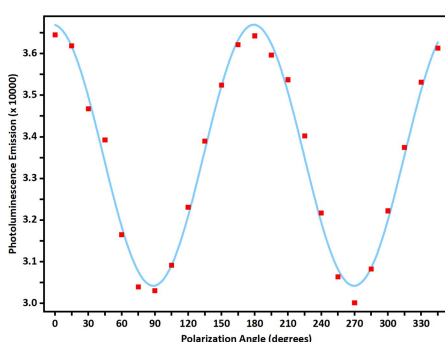
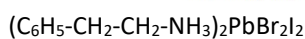
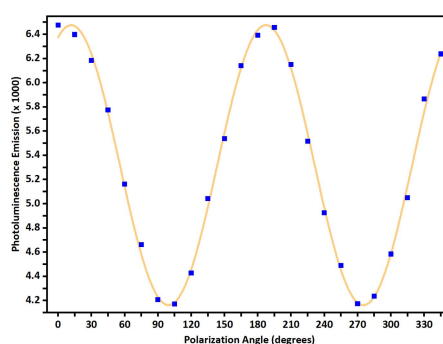
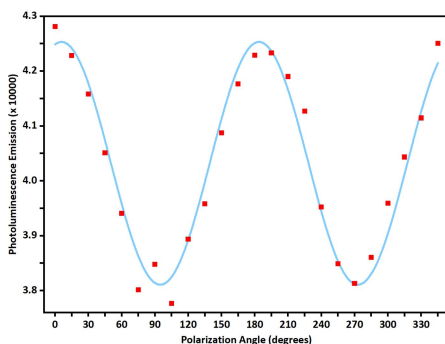
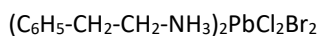
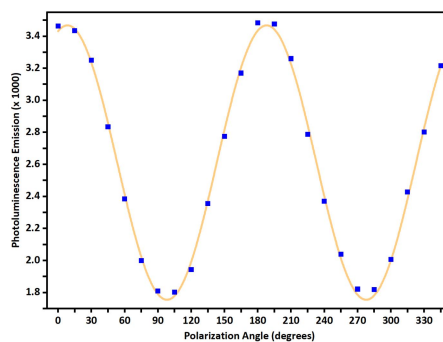
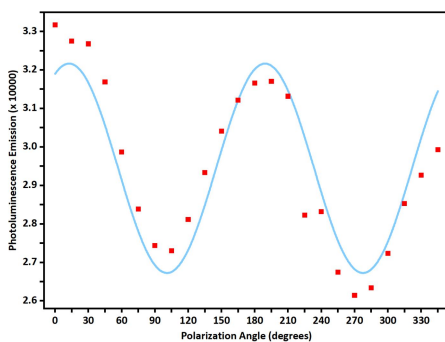
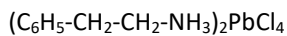


**Figure S16.** Linearly polarized photoluminescence (the left column) and polarization-dependent light-responsiveness (the right column) of colloidal liquid crystalline dispersions of  $(\text{C}_6\text{H}_5\text{-CH}_2\text{-CH}_2\text{-NH}_3)_2\text{PbCl}_4$ ,  $(\text{C}_6\text{H}_5\text{-CH}_2\text{-CH}_2\text{-NH}_3)_2\text{PbCl}_2\text{Br}_2$ ,  $(\text{C}_6\text{H}_5\text{-CH}_2\text{-CH}_2\text{-NH}_3)_2\text{PbBr}_2\text{I}_2$ , and  $(\text{C}_6\text{H}_5\text{-CH}_2\text{-CH}_2\text{-NH}_3)_2\text{PbBrI}_3$  perovskite nanoplatelets (from top to bottom).

**Table S1.** Degree of polarization values of colloidal liquid crystalline dispersions of perovskite nanoplatelets.

	Polarized Photoluminescence Light Emission	Polarization-Dependent Light-Responsiveness
$(\text{C}_6\text{H}_5\text{-CH}_2\text{-CH}_2\text{-NH}_3)_2\text{PbCl}_4$	0.12	0.32
$(\text{C}_6\text{H}_5\text{-CH}_2\text{-CH}_2\text{-NH}_3)_2\text{PbCl}_2\text{Br}_2$	0.06	0.22
$(\text{C}_6\text{H}_5\text{-CH}_2\text{-CH}_2\text{-NH}_3)_2\text{PbBr}_2\text{I}_2$	0.10	0.27
$(\text{C}_6\text{H}_5\text{-CH}_2\text{-CH}_2\text{-NH}_3)_2\text{PbBr}_1\text{I}_3$	0.08	0.24